Synergy of Low-Energy {101} and High-Energy {001} TiO_2 Crystal Facets for Enhanced Photocatalysis

Nitish Roy,[†] Youngku Sohn,[‡] and Debabrata Pradhan[†,*]

[†]Materials Science Centre, Indian Institute of Technology, Kharagpur 721 302, W.B., India and [‡]Department of Chemistry, Yeungnam University, Gyeongsan, Gyeongbuk 712-749, Korea

ABSTRACT Controlled crystal growth determines the shape, size, and exposed facets of a crystal, which usually has different surface physicochemical properties. Herein we report the size and facet control synthesis of anatase TiO_2 nanocrystals (NCs). The exposed facets are found to play a crucial role in the photocatalytic activity of TiO_2 NCs. This is due to the known preferential flow of photogenerated carriers to the specific facets. Although, in recent years, the main focus has been on increasing the surface area of high-energy exposed facets such as {001} and {100} to improve the photocatalytic activity, here we demonstrate that the presence of both the high-energy {001} oxidative and low-energy {101} reductive facets in an optimum ratio is necessary to reduce the charge recombination and thereby enhance photocatalytic activity of TiO_2 NCs.

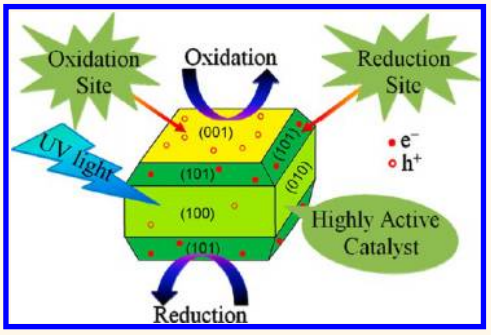

KEYWORDS: TiO_2 nanocrystals · facets control · photocatalysis · oxidation site · reduction site

Design and fabrication of TiO_2 nanostructures have attracted much attention because of their extensive uses in photocatalysis,[1−3] dye-sensitized solar cells,[4−6] self-cleaning agents,[7−9] electronic devices,[10] hydrogen production,[11,12] and supercapacitors.[13] The properties of nanomaterials are known to vary with the shape and size, which thereby have strong implications on their performances in potential applications. In the solution-based synthesis process, anatase TiO_2 crystals grow as truncated tetragonal bipyramidal shapes enwrapped with a large area of thermodynamically stable low-energy {101} and a small area of high-energy {001} exposed facets.[14] The high surface energy of {001} facets is considered to be due to the 100% 5-fold-coordinated titanium atoms (Ti_{5c}) as compared to 50% Ti_{5c} on the {101} surface.[15,16] Moreover, {010}/{100} facets also have 100% Ti_{5c} atoms, making it as another reactive facet.[14,17] The order of the average surface energies is as follows: γ{001} (0.90 J/m^2) > γ{100} (0.53 J/m^2) > γ{101} (0.44 J/m^2).[18] Thus extensive efforts have been made to synthesize TiO_2 crystals with a large area of high surface energy facets, particularly {001} facets.[14,19,20] Yang *et al.* successfully synthesized micrometer-size TiO_2 crystals with exposed {001} facets using hydrofluoric (HF) acid as a capping and shape-controlling agent.[21] Thenceforth several reports demonstrated the synthesis of shape-controlled TiO_2 crystals using HF.[16,20,22−25] However, HF is an environmentally unfriendly and extremely corrosive chemical. Therefore it is desirable to synthesize TiO_2 crystals with exposed reactive facets using a fluorine-free process. Recently, TiO_2 nanocrystals (NCs) with diverse shapes have been synthesized using a fluorine-free strategy.[14,26−28] However there is no report on the fine control of different facets of cuboid TiO_2 NCs using any synthesis technique. Herein, we demonstrate the fine control of different facets of cuboid TiO_2 NCs by varying the reaction duration using a fluorine-free shape-controlling reagent, *i.e.*, diethanolamine (DEA).

Although {001} and {100}/{010} facets of TiO_2 crystals are known as the most reactive and energetic facets because of their high surface energy,[21,24,29] their sole role in heterogeneous photocatalysis is still ambiguous.[23] Recently, Pan *et al.* confuted

* Address correspondence to deb@matsc.iitkgp.ernet.in.

Received for review December 19, 2012 and accepted February 28, 2013.

Published online February 28, 2013
10.1021/nn305877v

that the high-energy {001} TiO_2 facets are the reason behind the photocatalytic efficiency of TiO_2 NCs.[16] They showed that {010} facets have the highest photoreactivity and explained it on the basis of the cooperative mechanism of surface atomic structure (the density of undercoordinated Ti atoms) and surface electronic structure (the power of photoexcited charge carriers). One of the main aspects of photocatalytic activity is to reduce the recombination of photogenerated carriers. It has been found that anisotropic semiconducting crystals have a lower charge recombination than that of spherical particles.[30,31] This is due to the spontaneous separation of charge carriers toward different crystal facets.[32] In the case of anatase TiO_2, {001} and {101} facets have been demonstrated as oxidative and reductive sites, respectively, by single-molecule fluorescence probe[33] and photochemical deposition study.[34] Further, Liu *et al.* recently confirmed the improved photogenerated carrier separation by selectively depositing Pt on the exposed {101} facets.[35] Theoretical studies by Li *et al.* report detailed comparisons on the effect of shape, size, and surface structure on the photocatalytic behavior of anatase TiO_2 in an aqueous environment.[36−38] Therefore, it is important to explore the effect of physicochemical properties of different facets of TiO_2 NCs and their exact role in the photocatalytic behavior.

In the present work, in addition to the size-controlled synthesis of TiO_2 NCs, we synthesized NCs with either entirely high-energy {001} and {100}/{010} exposed facets or low-energy {101} exposed facets, or with a different percentage of {001}, {100}/{010}, and {101} facets. Then we demonstrate that not only more reactive {001} and {100}/{010} facets but also the presence of less reactive {101} facets are important for the improved photocatalysis. This is because of the preferential carrier transport to different facets of the TiO_2 crystal, thereby reducing the charge recombination.[32,33] The photocatalytic property of as-synthesized TiO_2 NCs is studied by the degradation of an organic contaminant in the presence of ultraviolet (UV) light.

RESULTS AND DISCUSSION

Surface Morphology. Figure 1 shows the field-emission scanning electron microscope (FE-SEM) images of TiO_2 NCs obtained by the hydrothermal synthesis method at 225 °C by varying the reaction duration (12 to 72 h) using titanium tetraisopropoxide (TTIP, 3 mmol) as a precursor and diethanolamine (20 mL, 200 mmol) and tetrabutylammonium hydroxide (TBAH, 20 mL, 80 mmol) as solvents. Here, DEA and TBAH are used as a shape-controlling agent and a bridging ligand, respectively. Insets of Figure 1a−e show the respective magnified FE-SEM images. The surface morphology of TiO_2 NCs is found to be uniform throughout the product, and their size distribution varied from smaller to larger with an increase in the

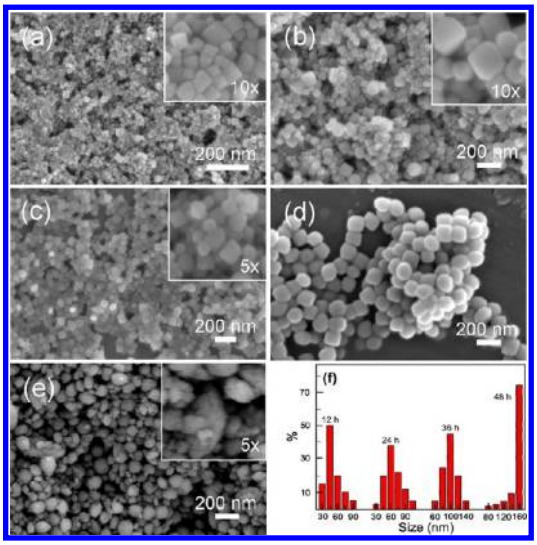

Figure 1. FE-SEM images of TiO_2 NCs obtained in (a) 12 h, (b) 24 h, (c) 36 h, (d) 48 h, and (e) 72 h, using the hydrothermal synthesis. Insets show the magnified FE-SEM images of the respective samples. (f) Size distribution of TiO_2 NCs obtained with different reaction durations.

reaction duration of the hydrothermal synthesis, as shown in Figure 1f. Figure 1a shows an FE-SEM image of TiO_2 NCs of size in the range 30−100 nm across the diagonal obtained in 12 h. In this case, the percentage of smaller TiO_2 NCs of size 30−50 nm (65%) is found to be higher than that of larger TiO_2 NCs (50−100 nm) (Figure 1f). Magnified images show these TiO_2 NCs are near-perfect cube-shaped. With increasing the reaction duration to 24 h (Figure 1b), the density of smaller TiO_2 NCs is found to be decreased, whereas the density of larger TiO_2 NCs (50−110 nm) increased. The magnified image in the inset of Figure 1b shows the reduction in sharpness on the edges and corners of these cube-like (cuboid) NCs. Figure 1c shows the cuboid TiO_2 NCs obtained in 36 h reaction. In this case a maximum percentage of cuboid TiO_2 NCs (45%) is found in the size range of 80−120 nm, which is larger than that for the NCs obtained in 12 and 24 h. On further increasing the reaction duration to 48 h, not only is the average size of cuboid TiO_2 NCs found to be increased, but also they have a narrow size distribution; 80% cuboid TiO_2 NCs are in the size range of 150 to 170 nm. Besides the size, it is also important to note the change in the shape of the cuboid TiO_2 NCs on increasing the reaction duration. Upon careful observation, it is noticed that the sharp edges of TiO_2 NCs become blurry and flattened with increasing the reaction duration of the synthesis. This suggests that the reaction duration plays an important role in the shape, size, and distribution of TiO_2 NCs. However, the synthesis performed for 72 h produced ellipsoid and distorted cuboid TiO_2 NCs, as shown in Figure 1e. The length and width of these ellipsoids are measured to be 100−350 nm and 80−250 nm, respectively. The distorted cuboid TiO_2 NCs are found in the size range of

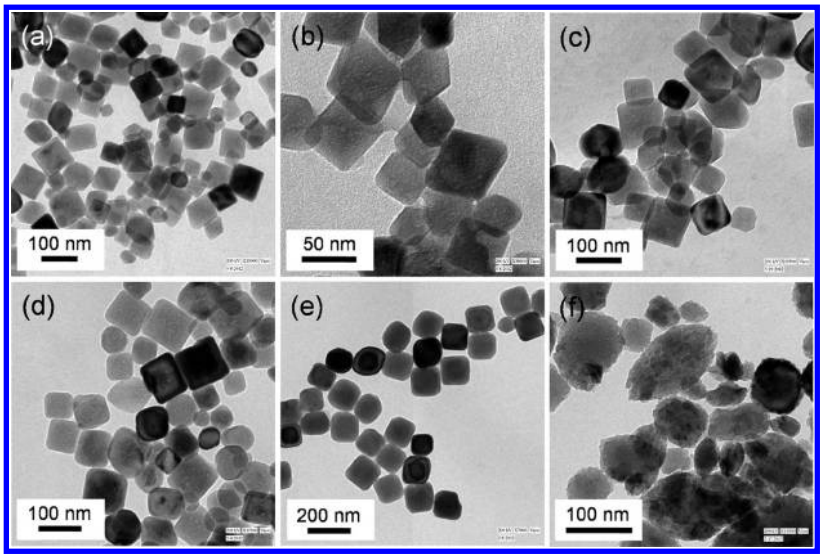

Figure 2. TEM images of TiO_2 NCs synthesized by hydrothermal process at 225 °C with a reaction duration of (a, b) 12 h, (c) 24 h, (d) 36 h, (e) 48 h, and (f) 72 h.

80−200 nm. These results show that an optimum reaction duration of 48 h is the most suitable to obtain uniformly sized cuboid TiO_2 NCs, whereas with 12 h reaction duration near-perfect cubic TiO_2 NCs can be obtained. It is important to compare the morphology of DEA-capped with the traditional fluorine (F)-capped TiO_2 crystals. The F-capping is normally achieved using HF, and it produces TiO_2 crystals in the shape of either truncated tetragonal bipyramids mainly with exposed low-energy {101} facets or nanosheets primarily with exposed high-energy {001} facets depending on the quantity of HF used in the synthesis.[16,19−21,39] A higher quantity of HF produces nanosheets due to the efficient capping of {001} facets.[19,39] The size of the truncated tetragonal bipyramids is reported to vary in the range of 1 to 3 μm, whereas the nanosheets are in the range of 10−1000 nm (length) and 3−260 nm (thickness).[16,19−21,39] On the other hand, in the present work we demonstrate cuboid TiO_2 NCs in the size range of 30−170 nm using DEA as an efficient capping agent. Furthermore, the molar concentration of DEA is found to play an important role in the morphology of TiO_2 NCs. At a very low (DEA:TBAH = 1:10) and high (DEA:TBAH = 10:1) DEA molar concentration, ellipsoid-like crystals [Supporting Information (SI), Figure S1(a)] and nanosheets [SI, Figure S1(b)] are obtained at 225 °C in 24 h of hydrothermal synthesis, respectively.

Microstructure and Structural Properties. Figure 2 shows the transmission electron microscope (TEM) images of TiO_2 NCs synthesized by the hydrothermal process at 225 °C by varying the reaction duration. The TEM images of the sample obtained in 12 h (Figure 2a,b) show cubic TiO_2 NCs with sharp edges and corners. The size of cubic TiO_2 NCs varies from 30 to 80 nm along the diagonal of the cubes. With an increase in the reaction duration to 24 h (Figure 2c) and 36 h (Figure 2d), the average size of the TiO_2 NCs increases to 50−110 nm and 60−120 nm, respectively. With a further increase in reaction duration to 48 h (Figure 2e), the average size of the cuboid TiO_2 NCs increases to the size range of 150−170 nm along with a narrow size distribution. The increase of size and improvement in the size distribution of cuboid TiO_2 NCs with an increase in reaction duration from 12 h to 48 h are in good agreement with FE-SEM analysis. Furthermore, the edges of TiO_2 NCs are found to be flattened with an increase in the reaction duration. Ellipsoid and distorted cuboid TiO_2 NCs obtained in 72 h are shown in Figure 2f. The length and width of ellipsoid NCs are measured to be 100−350 nm and 80−250 nm, respectively.

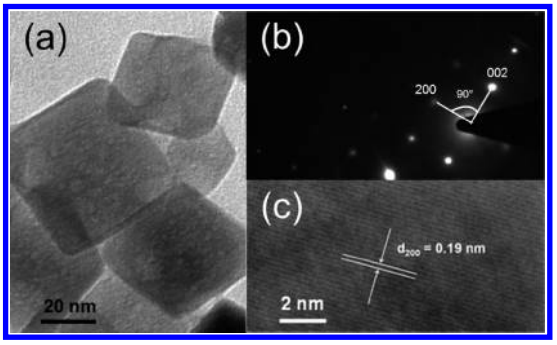

Figure 3. (a) TEM image of cubic TiO_2 NCs obtained in 12 h showing their sharp edges, (b) SAED spots of cubic TiO_2 NCs showing the diffracted planes and angle between them, and (c) the corresponding lattice fringe matching the distance between (200) planes of bulk TiO_2 crystals.

Figure 3a,b show the magnified TEM image and the corresponding selected area electron diffraction (SAED) pattern of near-perfect cubic TiO_2 NCs obtained in 12 h of hydrothermal reaction, respectively. The diffraction pattern of bright intense spots indicates the single-crystalline nature of the TiO_2 NCs. The absence of (101) planes in the SAED pattern indicates that the cubic TiO_2 NCs are surrounded by high-energy {001}

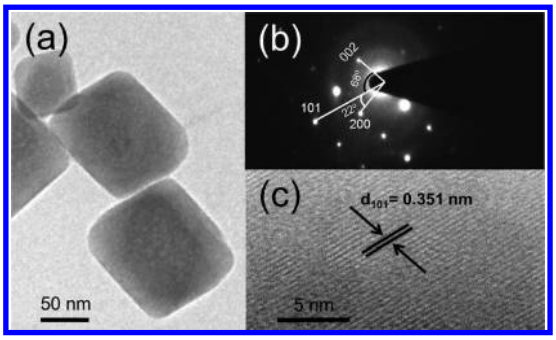

Figure 4. (a) TEM image of cuboid TiO_2 NCs obtained in the reaction duration of 36 h, (b) SAED spot pattern of the corresponding sample showing the diffracted planes and angle between them, and (c) the corresponding lattice fringe from the edge of a NC matches the spacing between (101) planes of bulk TiO_2 crystals.

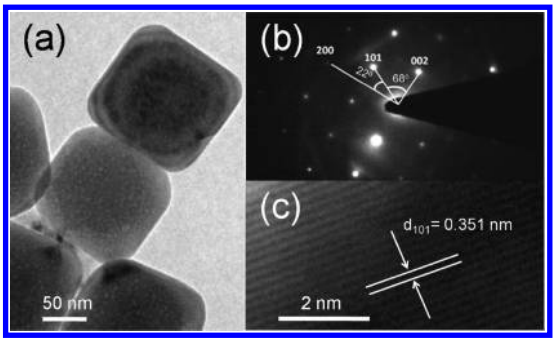

Figure 5. (a) TEM image of cuboid TiO_2 NCs obtained in the reaction duration of 48 h, (b) SAED spot pattern of the corresponding sample showing the diffracted planes and angle between them, and (c) the corresponding lattice fringe matching the distance between (101) planes of bulk TiO_2 crystals.

and {100} facets. The angle between different planes as designated in Figure 3b exactly matches the theoretical values.[25] Figure 3c shows a lattice image taken from the edge of a cube. The distance between two consecutive planes is measured to be 0.19 nm, which corresponds to the distance between (200) planes of anatase TiO_2. Thus the high-resolution TEM (HRTEM) study clearly suggests that the cubic TiO_2 NCs obtained in 12 h are solely enclosed by high-energy {001} and {100} facets.

Figure 4a,b show the magnified TEM and SAED pattern of cuboid TiO_2 NCs obtained in 36 h of hydrothermal reaction. The different crystal planes shown in Figure 4b are matched to the theoretical values.[25] The SAED spots clearly suggest the presence of low-energy {101} facets, indicating incorporation of {101} facets into the TiO_2 NCs. The lattice fringe taken from the edge of a cuboid TiO_2 NC shows the distance between two consecutive planes (Figure 4c). The measured lattice spacing of 0.351 nm indicates the presence of {101} facets at the edges of TiO_2 NCs synthesized in 36 h of hydrothermal reaction.

Figure 5a,b show the magnified TEM and SAED pattern of cuboid TiO_2 NCs obtained in 48 h of hydrothermal reaction. The contrast difference between the central and periphery part of the NCs indicates blunting at the edges of NCs, which is due to the incorporation of {101} facets. Incorporation of {101} facets reflects in their SAED pattern (Figure 5b) and lattice fringe taken from the edge of a cuboid NC (Figure 5c). The angles between the planes are found to exactly match the angles between (101) and (002), and (200) and (101) planes, as shown in Figure 5b. The distance between the two consecutive planes from the edge of a NC is measured to be 0.351 nm from the lattice image, which matches the distance between two consecutive (101) planes of bulk TiO_2, indicating that the edges of NCs have mainly {101} exposed facets.

In order to have a clear view of edges, corners, and facets of the as-synthesized TiO_2 NCs at different durations, we display the magnified FE-SEM image, TEM image, and schematic of the corresponding NCs in Figure 6. Near-perfect cube-shaped TiO_2 NCs (Figure 6a,b) with wholly high-energy {001} and {100}/{010} exposed facets are obtained in 12 h, which is in accord with their HRTEM analysis (Figure 3b,c). With an increase in the reaction duration to 24 h, the {101} facets are found to evolve along with the decrease in the surface area of exposed {100} facets (Figure 6c,d). On further increasing the reaction durations to 36 and 48 h, exposed area of {101} facets increases and that of the {100} facets decreases, as shown in Figure 6e,f and 6g,h, respectively. The relative surface area of different exposed facets of individual TiO_2 NCs was carefully calculated on the basis of magnified FE-SEM images and are presented in Table 1. The surface area of {101} facets of individual TiO_2 NCs increases from 0 to 32%, whereas that of {100} facets decreases from 58% to 33% with an increase in reaction duration from 12 h to 48 h. On the other hand, the surface area of the {001} facets of individual TiO_2 NCs remains almost the same, irrespective of the reaction duration.

The structural properties of TiO_2 NCs were investigated using an X-ray diffraction (XRD) study. Figure S2 shows the XRD patterns of TiO_2 NCs prepared in 12, 24, 36, 48, and 72 h. The sharp diffraction features obtained from the as-prepared samples clearly indicate the crystalline nature of TiO_2 NCs, and the 2θ diffraction positions are matched to the powder anatase TiO_2 of the tetragonal crystal system. The individual diffraction features are assigned as per JCPDS card no. 00-002-0387. The relative peak height of the (200) planes is found to increase with an increase in the reaction duration of TiO_2 NCs synthesis. This increase in relative intensity indicates the greater growth of cuboid TiO_2 NCs along the [100] direction and thereby the decrease in the exposed nature of the same facets with reaction duration. However, the XRD pattern obtained from the ellipsoid TiO_2 NCs formed in 72 h shows a mixed phase, *i.e.*, a minor rutile and a major anatase phase.

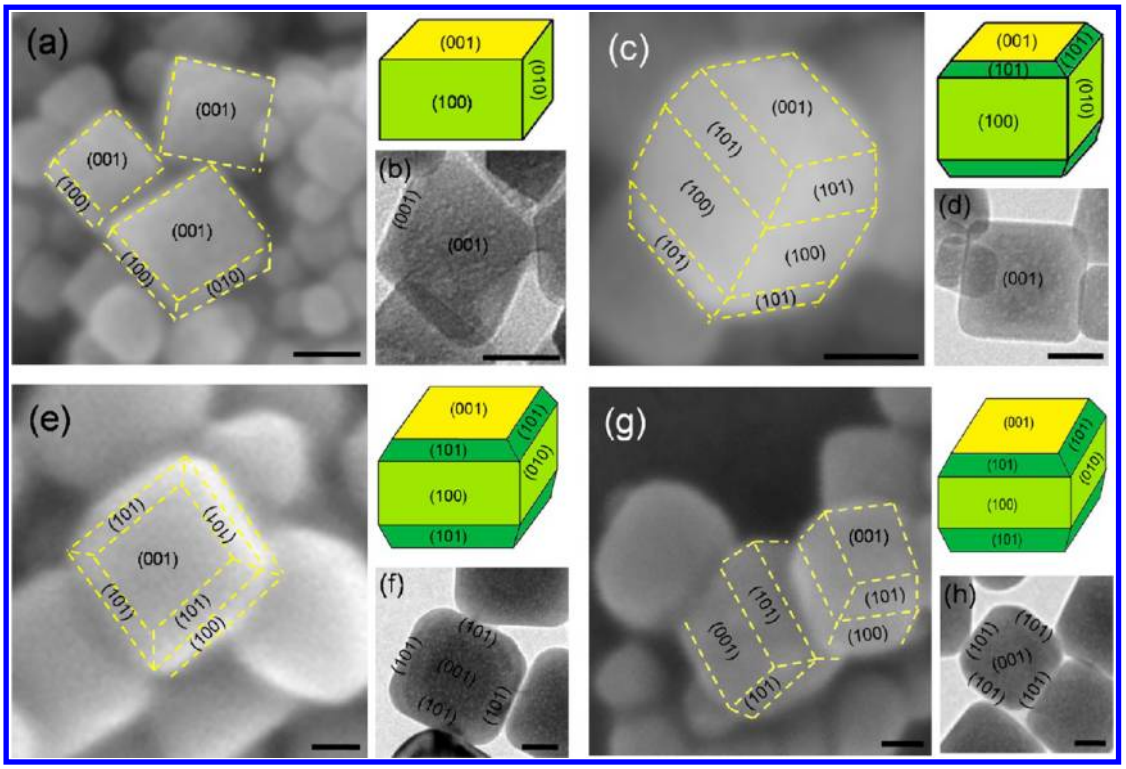

Figure 6. Magnified FE-SEM images, TEM images, and schematics of respective TiO_2 NCs are shown with different facets hydrothermally synthesized in (a, b) 12 h, (c, d) 24 h, (e, f) 36 h, and (g, h) 48 h. The length of scale bar in all the images is 25 nm.

TABLE 1. Exposed Related Surface Area of Different Facets of Individual Cuboid TiO_2 NCs Obtained with Different Reaction Duration

reaction duration	% of {101} facets	% of {001} facets	% of {100} facets
12 h	0	42	58
24 h	16	38	46
36 h	27	35	38
48 h	32	35	33

The diffraction peak at 2θ of 30.8° for the rutile phase is marked with ★ symbol.

Growth Mechanism. In the current work, the exposed facets of cuboid TiO_2 NCs was controlled by varying the reaction duration, keeping other parameters such as reaction temperature and initial molar concentrations of precursor, DEA, and TBAH fixed. For the synthesis of TiO_2 NCs, precursors play an important role. As the titanium alkoxide precursors (titanium isopropoxide or isobutoxide) are highly reactive toward moisture, the control of crystal growth is somewhat difficult in the aqueous medium.[14,40] Therefore, suitable organic solvents can be chosen not only to control the shape, facets, and size of TiO_2 NCs but also to obtain NCs with narrow size distribution and high crystallinity.[14,41,42] The amine compounds are widely used for fabricating the highly crystalline controlled morphology of TiO_2 NCs.[43,44] The amines have dual functions, *i.e.*, as a bridging ligand facilitating the formation of the Ti−O−Ti skeleton in a particular direction, and as a capping agent inhibiting the formation of the Ti−O−Ti skeleton three dimensionally. We chose DEA as a capping/shape-controlling agent because the optimized structure of DEA as per density functional theory (DFT) calculations (SI, Figure S3) shows that the distance between ammine-H and hydroxyl-H (0.46 nm) is closer to the distance between two consecutive 2c-O of {001} facets (0.53 nm) than the distance between two consecutive 2c-O of {101} facets (0.28 nm) of a TiO_2 surface.[24,25,45] Thus it is obvious that DEA can easily stabilize the {001} facets of TiO_2 exclusively through H-bonding. Such H-bonding onto {001} of TiO_2 NCs can hinder the growth along [001] and thereby expose the thermodynamically unstable energetic {001} facets. The hydrothermal reaction duration plays a crucial role in controlling the different facets of cuboid TiO_2 NCs. In the hydrothermal reaction, initially there was a sufficient quantity of DEA to cap the energetic {001} facets, which wholly exposes {001} and {100}/{010} facets, forming near-perfect cubic TiO_2 NCs in 12 h of reaction time (Figures 1a and 2a,b). However, with an increase in reaction duration, the thermodynamically more stable {101} facets start to evolve and the relative area of the {100}/{010} exposed facets decreases as these reactive {100}/{010} facets are not well capped by DEA. Further increasing the reaction duration to 72 h leads to NCs with primarily exposed {101} facets with ellipsoid shape. Thus keeping the initial concentration of DEA (capping agent) and other parameters fixed, the increase in reaction duration

leads to control of the different exposed facets of TiO_2 NCs.

Photocatalytic Properties. The principle of dye degradation by TiO_2 is based on a solid−liquid surface phenomenon assisted by UV light irradiation. The UV light creates electron/hole (e^-/h^+) pairs within the semiconductor. The generated e^-/h^+ pairs are effective in the photocatalysis only until their recombination. Therefore, the surface of a catalyst plays an important role in not allowing the recombination of photogenerated e^-/h^+ pairs. The different chemical environment of TiO_2 NCs facets makes it a unique material toward photocatalytic activity. On the basis of the DFT calculations combined with the periodic continuum solvation model, Li *et al*. reported that morphology-dependent photocatalytic activity of the sharp crystals was much higher than that of the flat crystals in an oxygen evolution reaction, which is due to the unique spatial separation/localization of the frontier orbitals in the sharp nanoparticles.[36] The theoretical results suggested that photocatalytic activity can be enhanced *via* nanostructure engineering.[36] In addition, they reported photocatalytic activity is strongly influenced by the energy position of the maximum of the valence band and the minimum of the conduction band. The anatase (101) surface has a stronger ability to accumulate photoelectrons than the 0.5 ML H_2O-covered (001) surface, suggesting the photocatalytic reduction process is favored on the (101) surface. However, the electronic structures at the maximum of the valence band are very similar for the (101) and the H_2O-covered (001) surfaces.[37] The surface chemical and electronic properties of TiO_2 NCs can be changed by tuning the relative ratios of exposed facets, *e.g.*, {101}, {001}, and {100}/{010}.[16] TiO_2 NCs dominated by {001} facets are known to show an enhanced photocatalytic property due to their high surface energy.[19,20,22] However it remains questionable whether the presence of only {001} and {100}/{010} facets can show enhanced photocatalytic activity.[16,20,45]

Figure 7 shows the extent of photodegradation of methyl orange (MO) by TiO_2 NCs obtained at different hydrothermal reaction durations. Capping agents such as fluorine and amine on the TiO_2 surface are known to influence the photocatalytic behavior.[14,16,20,46] Therefore, the as-synthesized TiO_2 NCs were first washed with 0.1 N HCl and then calcined at 400 °C in air for 2 h to remove the organic moieties (*i.e.*, DEA) capped on the NCs in order to determine the exact photocatalytic activity of different facets of TiO_2 NCs. The X-ray photoelectron spectroscopic (XPS) study reveals the presence and absence of the N 1s peak in the as-synthesized and after-treatment sample (SI, Figure S4), respectively. This suggests that acid washing and calcination completely removed the organic moieties from the TiO_2 surface. Prior to the photocatalysis, the

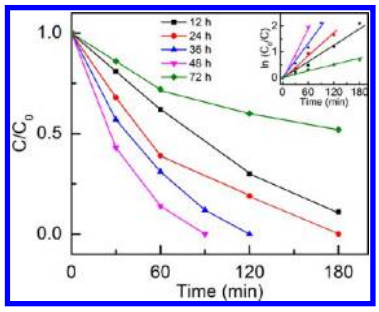

Figure 7. UV-light-assisted photodegradation of MO by TiO_2 NCs prepared with different reaction durations as a function of irradiation time. Inset graph shows the linear fitting curve of MO degradation.

catalyst−dye solution was kept in the dark for 30 min to completely saturate the dye adsorption on the TiO_2 surface [SI, Figure S5(a)]. Figure S5(b−f) shows the UV−vis absorption plots of MO as a function of irradiation time with the TiO_2 NCs obtained at different hydrothermal reaction durations. The MO degradation activity is low, with near-perfect cubic TiO_2 NCs even though having primarily high-energy exposed {001} and {100}/{010} facets, obtained in 12 h (Figures 1a and 2a,b), and also with ellipsoid NCs with exposed low-energy {101} facets, obtained in 72 h (Figures 1e and 2f), as shown in Figure 7. The MO degradation activity of cuboid TiO_2 NCs increases [even though the size of NCs increases and therefore the Brunauer−Emmett−Teller (BET) surface area decreases form 24.36 m^2/g (12 h) to 15.33 m^2/g (48 h)] with a gradual increase in the surface area of exposed low-energy {101} facets and becomes highest with the cuboid TiO_2 NCs obtained in 48 h (Figures 1d and 2e). The exposed surface area ratios of different facets were examined carefully, and it has been found that the cuboid TiO_2 NCs obtained in 48 h show approximately a 1:1 ratio of high-energy {001} and low-energy {101} facets (Table 1). The rate constants of MO degradation were estimated from the linearly fitted curve of $\ln(C_0/C)$ *vs* irradiation time, as shown in the inset of Figure 7, where "C_0" and "C" are the dye concentration before and after irradiation, respectively. The rate constant values are found to be $k_{12h} = 0.009$, $k_{24h} = 0.014$, $k_{36h} = 0.024$, $k_{48h} = 0.031$, and $k_{72h} = 0.004$ min^{-1}. Thus the highly active cuboid TiO_2 NC catalyst obtained in 48 h shows a 7.7 times higher rate of MO degradation than the TiO_2 NC catalyst obtained in 72 h. It is important to note that the BET surface areas of these cuboid TiO_2 NCs are much lower than that of a standard Degussa P25 photocatalyst (BET surface area ∼35−65 m^2/g) sample, and therefore a comparison is not made.[22]

Our present investigation shows that for improved photocatalysis an equal ratio of low-energy {101} and high-energy {001} facets is required. This is because of preferential flow of photogenerated holes and electrons to the oxidative {001} facets and reductive {101} facets, on which oxidation and reduction occur,

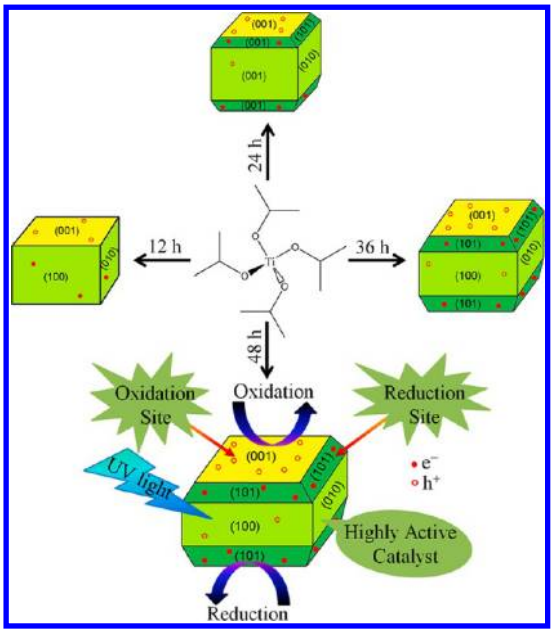

Figure 8. Schematic of TiO_2 NCs with different exposed facets. The surface area of exposed low-energy {101} facets is found to increase, while exposed high-energy {100}/{010} facets decrease with increase in the hydrothermal reaction duration, keeping other reaction parameters fixed (3 mmol TTIP, 225 °C, 5:2 DEA and TBAH molar ratio). The incorporation and increase in the surface area of reductive {101} facets leads to a decrease in charge recombination rate and becomes a minimum in the case of NCs obtained in 48 h.

respectively.[23,34,35,47] In particular, Maitani *et al.* have shown that the magnitude of electron transfer from anthracene derivatives to the {001} facet is 10 times larger than that to the {101} facets of TiO_2 NCs.[47] This clearly indicates that {001} facets are accumulated largely with positively charged holes as compared to {101} facets, thereby making {001} facets more active for photooxidation than the {101} facets. On the other hand, Wu *et al.* have shown an excess of electrons on the {101} facets and a lower recombination rate of e^-/h^+ pairs for the anisotropic TiO_2 NCs with {101} facets.[31] Liu *et al.* have also reported the highest activity for the TiO_2 crystals with Pt on the {101} facets. This was suggested to be due to the lower recombination rate of photogenerated e^-/h^+ pairs and excess negative charge on the {101} facets, favoring reduction. Although holes could be present on all the surfaces, the previous studies indicate a higher concentration of holes and electrons on the {001} and {101} facets, respectively.[32−35] Therefore, the presence of both the {001} and/or {100} facets (oxidation site) and {101} facets (reduction site) allows the photogenerated e^-/h^+ pairs to be separated for a longer duration and makes TiO_2 NCs more effective in the photocatalytic degradation of MO. Figure 8 shows the schematic representation of TiO_2 NCs with different exposed facets upon increasing the hydrothermal synthesis duration. The open and solid circles on the TiO_2 NCs (Figure 8)

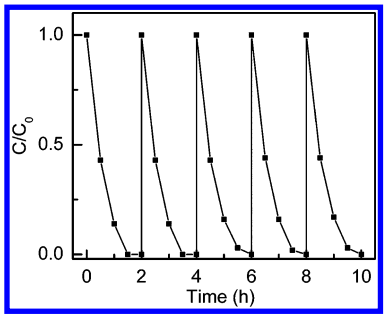

Figure 9. Efficiency of cuboid TiO_2 NCs obtained in 48 h of hydrothermal synthesis for the MO degradation *vs* UV irradiation duration with each run spanning 2 h.

indicate the excess holes and electrons on the respective facets. Irrespective of the small size (thereby larger BET surface area) and having wholly high-energy exposed facets, *i.e.*, {001} and {100}/{010}, the near-perfect cubic TiO_2 NCs obtained in 12 h show poor photocatalytic activity as compared to larger sized cuboid NCs obtained in 48 h. This is due to the absence of reductive {101} facets, which reduces the efficient charge separation ability in the near-perfect cube-shaped NCs. Similarly, the absence of {001} and/or {100}/{010} oxidative sites shows the lowest photocatalytic activity in the case of ellipsoid NCs with exposed {101} facets obtained in 72 h.

Durability Test. It is important to study the reliability and stability of a catalyst in prolonged use. Five runs of the MO degradation study were carried out for a constant 2 h irradiation time for each run with the catalyst obtained with 48 h reaction duration. Figure 9 shows the efficiency of TiO_2 NCs obtained in 48 h. There was only a slight decrease in MO degradation efficiency after the first cycle, and the efficiency of TiO_2 NCs remained almost the same for the rest of the four cycles (>96%), *i.e.*, after 30 min of UV irradiation in each cycle. This suggests that the activity and durability of as-synthesized TiO_2 NCs are high and not reduced even after 10 h of UV-light exposure.

CONCLUSIONS

This work reports a fluorine-free approach to prepare highly active anatase TiO_2 NCs with different percentages of exposed {101}, {001}, and {100}/{010} facets using DEA as a capping and facet-controlling agent. For the first time, we demonstrate a simple method to control the size and facets of cuboid TiO_2 NCs by varying the reaction duration. With increasing the reaction duration from 12 to 48 h, the size of cuboid TiO_2 NCs is found to increase from the range of 30−50 nm to 150−170 nm. The size distribution of cuboid TiO_2 NCs is also found to be narrower with increasing the reaction duration up to 48 h. The successive decrease in the exposed area of thermodynamically less stable {100} facets with reaction duration is due to the inefficient capping of less stable {100}

facets by DEA. Thus, reaction duration plays a crucial role in incorporating and successively increasing the exposed area of thermodynamically stable {101} facets. Increasing the reaction duration to 72 h produces ellipsoid TiO_2 NCs with primarily exposed {101} facets. The photocatalytic activity of {101} facets is found to be lowest among different facets of TiO_2 NCs and higher for {001} and/or {100}/{010} facets, but highest when both {101} and {001} and/or {100}/{010} facets are present with an equal ratio in the TiO_2 NCs. This brings us to conclude that the presence of low-energy {101} reductive facets is equally important along with {001} oxidative facets for efficient charge separation to enhance the photocatalytic activity. In addition to the removal of pollutants, these newly synthesized uniform cuboid TiO_2 NCs can find possible applications in dye-sensitized solar cells and hydrogen generation through water splitting.

EXPERIMENTAL DETAILS

Materials. All chemicals were analytical grade and used as received without further purification. Titanium tetraisopropoxide (99.999%), tetrabutylammonium hydroxide [$(C_4H_9)_4NOH$ in 0.1 N aqueous], and diethanolamine were purchased from Merck, India.

Synthesis of TiO_2 NCs. In a typical synthesis, 0.9 mL (3 mmol) of TTIP was added dropwise to a 40 mL mixture of TBAH (20 mL, 80 mmol) and DEA (20 mL, 200 mmol) at 2−5 °C. The transparent solution mixture of TBAH and DEA was observed to turn gummy white in the region where the TTIP drops fell, indicating the formation of a complex. The gummy, faintly precipitated solution was stirred for another 5 min. It was then brought to room temperature naturally and transferred into a 50 mL Teflon-lined autoclave. The autoclave was sealed and heated at 225 °C for different durations, *i.e.*, 12, 24, 36, 48, and 72 h, and cooled naturally to room temperature. The resulting reaction mixture was centrifuged to collect a white-colored TiO_2 powder, which was washed several times with DI water and ethanol. The white-colored product was dried in air for 24 h at 60 °C. In order to remove the organic moieties adsorbed on the TiO_2 surface during synthesis, first acid treatment (0.1 N HCl) was performed and subsequently calcination at 400 °C in air for 2 h in a Muffle furnace with a heating rate of 3 °C/min.

Characterization. The surface morphology of as-prepared TiO_2 powder was analyzed by a SUPRA 40 FE-SEM (Germany). The structural property of the samples was measured with a PANalytical high-resolution XRD, PW 3040/60 operated at 40 kV and 30 mA using Cu Kα X-rays. The detailed microstructure of the TiO_2 product was analyzed by using a TECNAI G2 TEM (FEI) and JEM-2100 HRTEM (JEOL) at an operating voltage of 200 kV. The surface composition of the TiO_2 NCs was characterized by XPS using a PHI 5000 VersaProbe II scanning XPS microprobe with a monochromatic Al Kα source (1486.6 eV).

Photocatalytic Study. The photocatalytic behavior of as-synthesized TiO_2 NCs was studied by degradation of MO dye in the presence of UV light. The dye solution was prepared by adding 40 mg of MO to 1 L of distilled water. Then 5 mL (50 μM) of MO dye stock solution was added to 45 mL of distilled water containing 20 mg of TiO_2 NCs and sonicated for 30 min in the dark at room temperature. The sample solution was then irradiated with a 6 W UV source (Philips, Poland) at a working distance of 10 cm from the light source for different durations to observe MO degradation using UV−visible absorption spectroscopy (PerkinElmer, Lambda 750).

Conflict of Interest: The authors declare no competing financial interest.

Acknowledgment. This work was supported by the Department of Science and Technology, New Delhi, India, through grant INT/Korea/P-02 and National Research Foundation of Korea, MEST (2012-0006296).

Supporting Information Available: TEM images; XRD patterns of TiO_2 NCs; schematic of electronic interaction between DEA and TiO_2 surface; XPS spectra; UV−vis absorption spectra of MO as a function of UV irradiation time in the presence of TiO_2 NCs synthesized by varying the reaction times. This material is available free of charge *via* the Internet at http://pubs.acs.org.

REFERENCES AND NOTES

1. Chowdhury, P.; Moreira, J.; Gomaa, J.; Ray, A. K. Visible-Solar-Light-Driven Photocatalytic Degradation of Phenol with Dye-Sensitized TiO_2: Parametric and Kinetic Study. *Ind. Eng. Chem. Res.* **2012**, *51*, 4523–4532.
2. Wang, C.; Zhang, X.; Zhang, Y.; Jia, Y.; Yang, Y.; Sun, P.; Liu, Y. Hydrothermal Growth of Layered Titanate Nanosheet Arrays on Titanium Foil and Their Topotactic Transformation to Heterostructured TiO_2 Photocatalysts. *J. Phys. Chem. C* **2011**, *115*, 22276–22285.
3. Liu, L.; Liu, H.; Zhao, Y. P.; Wang, Y.; Duan, Y.; Gao, G.; Ge, M.; Chen, W. Directed Synthesis of Hierarchical Nanostructured TiO_2 Catalysts and their Morphology-Dependent Photocatalysis for Phenol Degradation. *Environ. Sci. Technol.* **2008**, *42*, 2342–2348.
4. Kang, T. S.; Smith, A. P.; Taylor, B. E.; Durstock, M. F. Fabrication of Highly-Ordered TiO_2 Nanotube Arrays and Their Use in Dye-Sensitized Solar Cells. *Nano Lett.* **2009**, *9*, 601–606.
5. Kuang, D.; Brillet, J.; Chen, P.; Takata, M.; Uchida, S.; Miura, H.; Sumioka, K.; Zakeeruddin, S. M.; Gratzel, M. Application of Highly Ordered TiO_2 Nanotube Arrays in Flexible Dye-Sensitized Solar Cells. *ACS Nano* **2008**, *2*, 1113–1116.
6. Shankar, K.; Bandara, J.; Paulose, M.; Wietasch, H.; Varghese, O. K.; Mor, G. K.; LaTempa, T. J.; Thelakkat, M.; Grimes, C. A. Highly Efficient Solar Cells Using TiO_2 Nanotube Arrays Sensitized with a Donor-Antenna Dye. *Nano Lett.* **2008**, *8*, 1654–1659.
7. Wang, R. H.; Wang, X. W.; Xin, J. H. Advanced Visible-Light-Driven Self-Cleaning Cotton by Au/TiO_2/SiO_2 Photocatalysts. *ACS Appl. Mater. Interfaces* **2010**, *2*, 82–85.
8. Fateh, R.; Ismail, A. A.; Dillert, R.; Bahnemann, D. W. Highly Active Crystalline Mesoporous TiO_2 Films Coated onto Polycarbonate Substrates for Self-Cleaning Applications. *J. Phys. Chem. C* **2011**, *115*, 10405–10411.
9. Xi, B.; Verma, L. K.; Li, J.; Bhatia, C. S.; Danner, A. J.; Yang, H.; Zeng, H. C. TiO_2 Thin Films Prepared *via* Adsorptive Self-Assembly for Self-Cleaning Applications. *ACS Appl. Mater. Interfaces* **2012**, *4*, 1093–1102.
10. Dutta, S.; Patra, A. K.; De, S.; Bhaumik, A.; Saha, B. Self-Assembled TiO_2 Nanospheres by Using a Biopolymer as a Template and Its Optoelectronic Application. *ACS Appl. Mater. Interfaces* **2012**, *4*, 1560–1564.
11. Lin, W.-C.; Yang, W.-D.; Huang, I.-L.; Wu, T.-S.; Chung, Z.-J. Hydrogen Production from Methanol/Water Photocatalytic Decomposition Using Pt/TiO_2-xNx Catalyst. *Energy Fuels* **2009**, *23*, 2192–2196.
12. Bae, E.; Choi, W. Effect of the Anchoring Group (Carboxylate vs Phosphonate) in Ru-Complex-Sensitized TiO_2 on Hydrogen Production under Visible Light. *J. Phys. Chem. B* **2006**, *110*, 14792–14799.
13. Lu, X.; Wang, G.; Zhai, T.; Yu, M.; Gan, J.; Tong, Y.; Li, Y. Hydrogenated TiO_2 Nanotube Arrays for Supercapacitors. *Nano Lett.* **2012**, *12*, 1690–1696.
14. Wu, B.; Guo, C.; Zheng, N.; Xie, Z.; Stucky, G. D. Nonaqueous Production of Nanostructured Anatase with High-Energy Facets. *J. Am. Chem. Soc.* **2008**, *130*, 17563–17567.
15. Vittadini, A.; Selloni, A.; Rotzinger, F. P.; Gratzel, M. Structure and Energetics of Water Adsorbed at TiO_2 Anatase

(101) and (001) Surfaces. *Phys. Rev. Lett.* **1998**, *81*, 2954–2957.
16. Pan, J.; Liu, G.; Lu, G. Q.; Cheng, H.-M. On the True Photoreactivity Order of {001}, {010}, and {101} Facets of Anatase TiO_2 Crystals. *Angew. Chem., Int. Ed.* **2011**, *50*, 2133–2137.
17. Li, J. M.; Xu, D. S. Tetragonal Faceted-Nanorods of Anatase TiO_2 Single Crystals with a Large Percentage of Active {100} Facets. *Chem. Commun.* **2010**, *46*, 2301–2303.
18. Lazzeri, M.; Vittadini, A.; Selloni, A. Structure and Energetics of Stoichiometric TiO_2 Anatase Surfaces. *Phys. Rev. B: Condens. Mater. Phys.* **2002**, *65*, 119901.
19. Han, X.; Kuang, Q.; Jin, M.; Xie, Z.; Zheng, L. Synthesis of Titania Nanosheets with a High Percentage of Exposed (001) Facets and Related Photocatalytic Properties. *J. Am. Chem. Soc.* **2009**, *131*, 3152–3153.
20. Yang, H. G.; Liu, G.; Qiao, S. Z.; Sun, C. H.; Jin, Y. G.; Smith, S. C.; Zou, J.; Cheng, H. M.; Lu, G. Q. Solvothermal Synthesis and Photoreactivity of Anatase TiO_2 Nanosheets with Dominant {001} Facets. *J. Am. Chem. Soc.* **2009**, *131*, 4078–4083.
21. Yang, H. G.; Sun, C. H.; Qiao, S. Z.; Zou, J.; Liu, G.; Smith, S. C.; Cheng, H. M.; Lu, G. Q. Anatase TiO_2 Single Crystals with a Large Percentage of Reactive Facets. *Nature* **2008**, *453*, 638–641.
22. Liu, M.; Piao, L.; Zhao, L.; Ju, S.; Yan, Z.; He, T.; Zhoua, C.; Wang, W. Anatase TiO_2 Single Crystals with Exposed {001} and {110} Facets: Facile Synthesis and Enhanced Photocatalysis. *Chem. Commun.* **2010**, *46*, 1664–1666.
23. Fang, W. Q.; Gong, X. -Q.; Yang, H. G. On the Unusual Properties of Anatase TiO_2 Exposed by Highly Reactive Facets. *J. Phys. Chem. Lett.* **2011**, *2*, 725–734.
24. Selloni, A. Anatase Shows Its Reactive Side. *Nat. Mater.* **2008**, *7*, 613–615.
25. Nguyen, C. K.; Cha, H. G.; Kang, Y. S. Axis-Oriented, Anatase TiO_2 Single Crystals with Dominant {001} and {100} Facets. *Cryst. Growth Des.* **2011**, *11*, 3947–3953.
26. Han, X.; Wang, X.; Xie, S.; Kuang, Q.; Ouyang, J.; Xie, Z.; Zheng, L. Carbonate Ions-Assisted Syntheses of Anatase TiO_2 Nanoparticles Exposed with High Energy (001) Facets. *RSC Adv.* **2012**, *2*, 3251–3253.
27. Han, X.; Zheng, B.; Ouyang, J.; Wang, X.; Kuang, Q.; Jiang, Y.; Xie, Z.; Zheng, L. Control of Anatase TiO_2 NCs with a Series of High-Energy Crystal Facets *via* a Fluorine-Free Strategy. *Chem. Asian J.* **2012**, *11*, 2538–2542.
28. Dai, Y.; Cobley, C. M.; Zeng, J.; Sun, Y.; Xia, Y. Synthesis of Anatase TiO_2 NCs with Exposed {001} Facets. *Nano Lett.* **2009**, *9*, 2455–2459.
29. Lazzeri, M.; Vittadini, A.; Selloni, A. Structure and Energetics of Stoichiometric TiO_2 Anatase Surfaces. *Phys. Rev. B* **2001**, *63*, 155409.
30. Mor, G. K.; Shankar, K.; Paulose, M.; Varghese, O. K.; Grimes, C. A. Enhanced Photocleavage of Water Using Titania Nanotube Arrays. *Nano Lett.* **2005**, *5*, 191–195.
31. Wu, N. Q.; Wang, J.; Tafen, D.; Wang, H.; Zheng, J. G.; Lewis, J. P.; Liu, X. G.; Leonard, S. S.; Manivannan, A. Shape-Enhanced Photocatalytic Activity of Single-Crystalline Anatase TiO_2 (101) Nanobelts. *J. Am. Chem. Soc.* **2010**, *132*, 6679–6685.
32. Giocondi, J. L.; Salvador, P. A.; Rohrer, G. S. The Origin of Photochemical Anisotropy in $SrTiO_3$. *Top. Catal.* **2007**, *44*, 529–533.
33. Tachikawa, T.; Yamashita, S.; Majima, T. Evidence for Crystal-Face-Dependent TiO_2 Photocatalysis from Single-Molecule Imaging and Kinetic Analysis. *J. Am. Chem. Soc.* **2011**, *133*, 7197–7204.
34. Murakami, N.; Kurihara, Y.; Tsubota, T.; Ohno, T. Shape-Controlled Anatase Titanium(IV) Oxide Particles Prepared by Hydrothermal Treatment of Peroxo Titanic Acid in the Presence of Polyvinyl Alcohol. *J. Phys. Chem. C* **2009**, *113*, 3062–3069.
35. Liu, C.; Han, X.; Xie, S.; Kuang, Q.; Wang, X.; Jin, M.; Xie, Z.; Zheng, L. Enhancing the Photocatalytic Activity of Anatase TiO_2 by Improving the Specific Facet-Induced Spontaneous Separation of Photogenerated Electrons and Holes. *Chem. Asian J.* **2013**, *8*, 282–289.
36. Li, Y.-F.; Liu, Z.-P. Particle Size, Shape and Activity for Photocatalysis on Titania Anatase Nanoparticles in Aqueous Surroundings. *J. Am. Chem. Soc.* **2011**, *133*, 15743–15752.
37. Li, Y.-F.; Liu, Z.-P.; Liu, L.; Gao, W. Mechanism and Activity of Photocatalytic Oxygen Evolution Titania Anatase in Aqueous Surroundings. *J. Am. Chem. Soc.* **2010**, *132*, 13008–13015.
38. Li, Y.-F.; Liu, Z.-P. Dual Reaction Channels for Photocatalytic Oxidation of Phenylmethanol on Anatase. *Phys. Chem. Chem. Phys.* **2013**, *15*, 1082–1087.
39. Tian, F.; Zhang, Y.; Zhang, J.; Pan, C. Raman Spectroscopy: A New Approach to Measure the Percentage of Anatase TiO_2 Exposed (001) Facets. *J. Phys. Chem. C* **2012**, *116*, 7515–7519.
40. Chae, S. K.; Park, M. K.; Lee, S. K.; Kim, T. Y.; Kim, S. K.; Lee, W. I. Preparation of Size-Controlled TiO_2 NCs and Derivation of Optically Transparent Photocatalytic Films. *Chem. Mater.* **2003**, *15*, 3326–3331.
41. Niederberger, M.; Bartl, M. H.; Stucky, G. D. Benzyl Alcohol and Transition Metal Chlorides As a Versatile Reaction System for the Nonaqueous and Low-Temperature Synthesis of Crystalline Nano-Objects with Controlled Dimensionality. *J. Am. Chem. Soc.* **2002**, *124*, 13642–13643.
42. Kotsokechagia, T.; Cellesi, F.; Thomas, A.; Niederberger, M.; Tirelli, N. Preparation of Ligand-Free TiO_2 (Anatase) NCs through a Nonaqueous Process and Their Surface Functionalization. *Langmuir* **2008**, *24*, 6988–6997.
43. Dinh, C.-T.; Nguyen, T.-D.; Kleitz, F.; Do, T.-O. Shape-Controlled Synthesis of Highly Crystalline Titania NCs. *ACS Nano* **2009**, *11*, 3737–3743.
44. Chen, Q.; Mao, S. S. Titanium Dioxide Nanomaterials: Synthesis, Properties, Modifications, and Applications. *Chem. Rev.* **2007**, *107*, 2891.
45. Wang, L.; Zang, L.; Zhao, J.; Wang, C. Green Synthesis of Shape-Defined Anatase TiO_2 Nanocrystals Wholly Exposed with {001} and {100} Facets. *Chem. Commun.* **2012**, *48*, 11736–11738.
46. Liu, S.; Yu, J.; Jaroniec, M. Anatase TiO_2 with Dominant High-Energy {001} Facets: Synthesis, Properties, and Applications. *Chem. Mater.* **2011**, *23*, 4085–4093.
47. Maitani, M. M.; Tanaka, K.; Mochizuki, D.; Wada, Y. Enhancement of Photoexcited Charge Transfer by {001} Facet-Dominating TiO_2 Nanoparticles. *J. Phys. Chem. Lett.* **2011**, *2*, 2655–2659.